

Improved Calibration for an Experimental Time-Domain Microwave Imaging System

Adam Santorelli, Evgeny Kirshin, Emily Porter,
Milica Popović
Department of Electrical and Computer Engineering,
McGill University, Montreal, Canada

Joshua Schwartz
Department of Engineering Science,
Trinity University
San Antonio, Texas, United States of America

Abstract—In this paper, we investigate the use of several different materials in order to calibrate an experimental time-domain microwave imaging system. A 16-element antenna array transmits a specifically tailored, short duration pulse and records the signals scattered off the breast in the time-domain. We contrast the performance of the various calibration procedures on extracting the tumour response and locating the tumour embedded within realistically shaped life-like breast phantoms.

Index Terms— cancer detection; microwave imaging; multistatic radar; breast phantoms; pulse shaping; calibration;

I. INTRODUCTION

Microwave imaging systems offer the potential to be a complementary modality to X-ray mammography as an early-stage breast cancer screening technique. These techniques are safe (as there is no source of ionizing radiation), easy to operate, and unlike magnetic resonance imaging (MRI) they are cost effective, thus presenting a viable imaging technique for breast monitoring [1]. Due to the differences in dielectric properties of malignant and healthy breast tissue [1], incident electromagnetic waves in the microwave range undergo non-uniform scattering. These signals can be recovered and used for breast image reconstruction to identify the presence of malignant tissues within the breast.

To date, the predominant research focus has been on the development of experimental systems which perform measurements in the frequency domain, such as those in [2] - [6], with some of the systems, [2] - [3], undergoing clinical testing. However, a recent investigation into the accuracy of comparative time-domain systems reports that time-domain systems offer an advantage over frequency-domain techniques by decreasing the scan duration while also offering the potential for improved cost-effectiveness, with the trade-off being a decrease in the signal-to-noise ratio of the system [7].

In this paper we focus on a new procedure for calibrating our experimental time-domain measurement system. By performing measurements in the time-domain we are able to take advantage of the proposed benefits for time-domain systems outlined in [7].

II. BACKGROUND

A calibration procedure is necessary to extract the tumour response from the recorded data and to allow for successful imaging of the breast. A set of reference signals is recorded and subsequently used to remove the effects of the direct pulse

(signals travelling directly between nearest-neighbour antennas without passing through the breast), reflections from the antenna housing structure, and the early-time response due to the healthy tissues within the breast.

In frequency-domain systems this calibration procedure has been shown to be complex and time-consuming. For example, in [4] the calibration procedure requires first recording data from an empty breast immersion tank (to remove reflections from tank walls), then recording data when metal plates are inserted into the immersion tank in order to both confirm the permittivity of the immersion medium and to estimate the distance from antennas to the object being imaged; additionally, a laser is used to identify the breast surface shape. The clinically ready system presented in [2] uses a reference signal that is obtained by mechanically rotating the antenna array around the breast under examination. This procedure is dependent on knowing the exact degree to which the antenna array has been rotated with regards to the object under test, thus a highly precise motor is required. In [6], the calibration procedure makes use of two reference signals: a measured one, obtained from an empty antenna system (the object under test is removed from the system), and a matching simulated one, obtained using FDTD numerical simulations of the same empty antenna array system.

Experimental time-domain systems have mainly focused on differential calibration techniques, [8] - [10], in which a reference signal, obtained from a scan of a healthy breast, is used for calibration. The recorded data from the healthy scan is then subtracted from the most recent scan; any changes in the breast composition are represented in the differential signal. This differential calibration technique is not ideal for a clinical setting, as it requires previous knowledge of the breast; in order to obtain a healthy baseline the patient must be proclaimed to be cancer free (confirmed by another imaging technique).

We present a procedure to calibrate our experimental time-domain system that does not require a previous, healthy scan of the breast. We collect signals from three different materials, fat-mimicking tissue, ultrasound (US) gel, and safflower oil, to create a basic, preliminary library of reference signals to be used for calibration. Unlike the differential techniques, the calibration measurements only need to be performed once; they are not repeated for each individual phantom. We record data from realistically shaped life-like breast phantoms and compare the reconstructed images when using each of the three reference sets to calibrate the system. We then identify, based

This work was supported by the Natural Sciences and Engineering Research Council of Canada (NSERC), le Fonds québécois de la recherche sur la nature et les technologies (FQRNT) and Partenariat de Recherche Orientée en Microélectronique, Photonique et Télécommunications (PROMPT).

on the reconstructed images and the associated detection metrics provided, the calibration material that yields the most promising results. Finally, we demonstrate that calibration using a predefined data set offers good image quality and is without the associated drawbacks of differential calibration methods.

III. EXPERIMENTAL SYSTEM

The experimental system consists of a 16-element antenna array housed in a hemispherical bowl-shaped radome. The antennas used in the system are wideband, compact in size ($0.635 \times 12 \times 18 \text{ mm}^3$), and have been specifically designed for microwave imaging of the breast [8]; they have been designed for optimum performance ($S_{11} < -10 \text{ dB}$ from 3 - 12 GHz) when surrounded by a medium with properties similar to adipose breast tissue (relative permittivity $\epsilon_r \approx 9$). The radome serves as the interface between the system and the breast; the exterior surface has slots to hold the antennas in place, while the interior surface holds the breast in place. This rigid structure ensures that the antennas cannot move relative to the breast during a measurement. A commonly-used time-domain pulse, [7], [9], is reshaped using a planar microwave filter [11] to create a specifically tailored short duration pulse, with the majority of its signal content in the 2 - 4 GHz range.

This custom-made pulse is launched from a single transmit antenna and collected from the remaining 15 receiving antennas. A switching network, consisting of coaxial switches, is used to cycle through the 15 receiving antennas for each transmitter. This process is repeated for each transmitter, and, in total, 240 bistatic signals are collected for each scan. Signals are digitally recorded using an oscilloscope operating at an equivalent-time sampling rate of 80 GS/s. As demonstrated in [11], the reshaped pulse improves the tumour detection capabilities of our experimental system. A block diagram of the experimental system is shown in Fig. 1. A complete description of the experimental system, with thorough explanations of each system component, can be found in [8] and [11]. Currently, a complete scan can be completed in under 20 minutes.

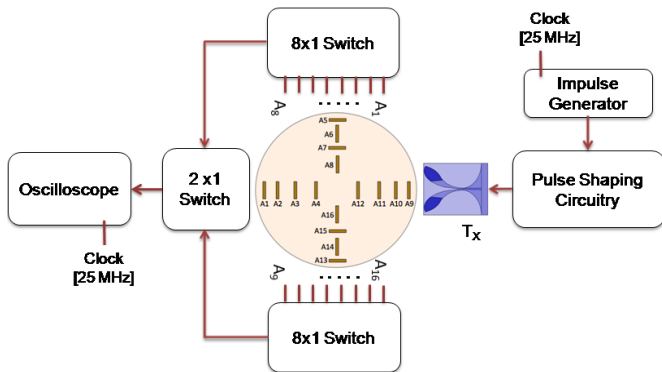


Figure 1. A high-level schematic of the experimental system. The 16 antenna slots of the radome are labelled, and an image of the antenna is depicted. The pulse-shaping circuitry refers to the system components needed to create the custom-shaped pulse.

IV. METHODOLOGY

In this section we proceed to describe the materials and methods that are necessary to implement the newly developed calibration procedure, as well as the steps required to collect the data from the breast phantoms in order to create the reconstructed images of the breast phantom interior.

A. Calibration Method

A set of reference signals from each of the three different materials is recorded to create a library of signals that can be used for calibration of the experimental system. These recordings are obtained by completely filling the radome with either the safflower oil, the US gel, or the fat-mimicking tissue and then collecting the 240 signals of a complete scan. A plot of the relative permittivity of each material is shown in Fig. 2. We also note that the safflower oil has the lowest loss, whereas the US gel, which behaves similarly to water, has the highest loss.

In order to properly calibrate the experimental system, the reference signals must first be time-aligned and then normalized. This procedure is necessary to remove the direct pulse and early-time response signal.

The time-alignment procedure is necessary to compensate for the effects of jitter arising in the experimental system (due to deviations in the control clock signal and the oscilloscope trigger). We implement two methods to overcome these effects. The first method, referred to here as a “reference alignment”, involves recording and aligning the clock signal that triggered the generated impulse for the received signals from different scans in the time-domain. The second method, referred to as a “correlation alignment”, aligns signals by identifying the time shift that leads to the best match between the signals. Fig. 3 depicts an example of the potential time delay, ΔT , between a reference and recorded signal. The time-alignment procedures are used to identify the value of this time-delay and shift the reference signal accordingly.

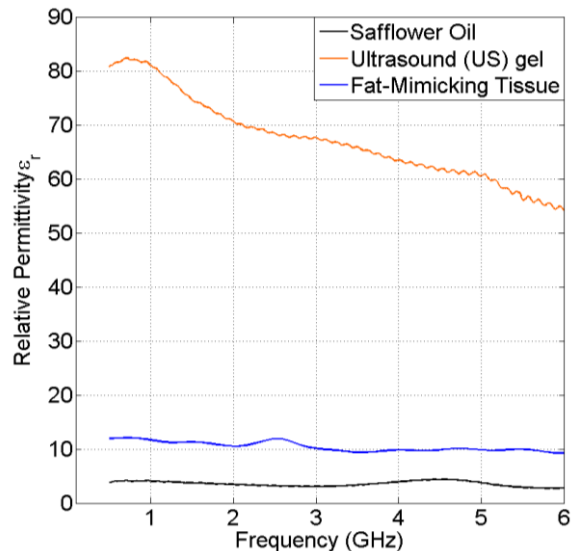


Figure 2. Relative permittivity of the calibration media over microwave frequencies.

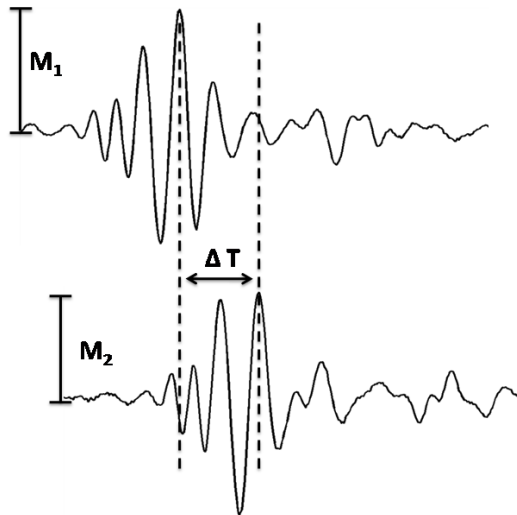


Figure 3. An example demonstrating the potential mismatch between the recorded signal from a breast scan and the corresponding reference signal. Here ΔT represents the delay between the two signals that is compensated for by the time-alignment procedure. M_1 and M_2 , respectively, represent the maximum signal amplitude for the recorded and reference signal.

A normalization procedure adjusts the amplitude of the direct pulse in the reference signal. Without this, the direct pulse residual, i.e. the signal that remains after using the reference signal to calibrate the system, would drown out the weaker tumour response, thereby making imaging impossible. A normalization factor, k , is found such that:

$$k = M_1/M_2 \quad (1),$$

where M_1 and M_2 are the maximum amplitudes of the direct pulse for the recorded and reference signals respectively, as shown in Fig. 3. The reference signal is then multiplied by this normalization factor.

The final step of the calibration procedure is to subtract the time-aligned and normalized reference signal from the recorded signal. An example of the resulting signal, referred to as the tumour response signal, is shown in Fig. 4. We highlight that the direct pulse has been successfully removed from the recorded signal and the tumour response remains unaffected by the calibration. The signals plotted in Fig. 4 were obtained when using the fat-mimicking tissue as the calibration medium for nearest-neighbour antennas with a 1-cm radius tumour embedded in the phantom.

B. Breast Phantom Data Collection

Data was recorded from realistically shaped breast phantoms made up of 100% adipose tissue with a 2-mm thick skin layer. A 1-cm radius, spherical tumour phantom is embedded into each phantom. The breast phantoms were made from easily obtainable chemicals and were fabricated to exhibit similar dielectric properties in the microwave range as real breast tissues [12]. Additionally, a reference signal was recorded from the tumour free phantoms, representing a healthy baseline, in order to compare the new calibration method with the differential method.

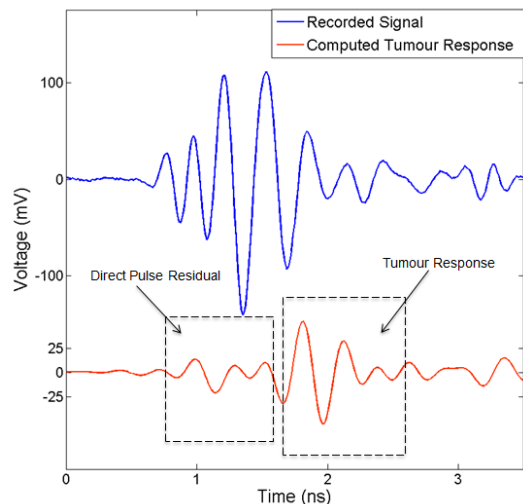


Figure 4. An example of the resulting tumour response signal after calibration. We highlight the direct pulse residual and the tumour response. This is an example of successful calibration as the direct pulse and the early-time response has been removed from the recorded signal while the tumour response is now revealed.

V. RESULTS

The calibration procedure is repeated for each of the recorded reference signals (healthy baseline, fat-mimicking tissue, US gel, and safflower oil). We reconstruct an image of the breast phantom under test by making use of the DMAS imaging algorithm [13] and applying it to the computed tumour response signals.

In Fig. 5, we compare coronal slices of the reconstructed 3-D images of the realistically shaped adipose breast phantom when using differential calibration (A), and the newly adopted calibration method outlined here within when using the fat-mimicking tissue (B) and the US gel (C) to collect the reference signals. In the images the ‘x’ markers denote antenna locations and the ‘◇’ symbol denotes the physical location where the tumour is inserted into the phantom. We note that in each image, red indicates strongly scattered electromagnetic energy. From these reconstructed images it is clear that both the differential-calibration method and the new calibration method using the fat-mimicking tissue are able to detect and identify the tumour as the maximum scatterer.

To assess the quality of the tumour detection we use the signal-to-clutter ratio (SCR) and the tumour localisation error metrics. The signal-to-clutter ratio is defined as the ratio between the intensity of the maximum scatterer (representing the tumour) and the next highest intensity (attributed to the clutter or healthy tissue in the breast phantom), and is commonly utilized in assessing the performance of microwave imaging systems [9], [14]. The tumour localisation error is defined as the distance from the maximum scatterer in the image to the centre of the embedded tumour. Table I compares these metrics for each of the three reconstructed images.

Based on the SCR, the differential method leads to the best result, however, using the new calibration method with the fat-mimicking tissue we obtain a result that is in line with those of [14], and better than the results reported in [9] (however this

study looked into heterogeneous breast phantoms). Additionally, the computed localisation error for the two methods is almost identical, and on the order of the size of the embedded tumour; we are able to locate the tumour to a distance less than its diameter. Thus, we have demonstrated that using the fat-mimicking tissue to record a set of reference signals to calibrate the experimental system when imaging a adipose breast phantom offers a successful method to bypass the need of having prior knowledge of the breast tissue; we have eliminated the major drawback of the differential method that requires a healthy scan as a baseline.

The use of the US gel as a material to obtain the reference signals does not lead to positive results. While the computed SCR is in line with expectations, it is clear from the reconstructed image that the tumour is detected at a location that is shifted from its actual location. A possible explanation as to why the fat-mimicking tissue seems to be the better choice for calibration can be attributed to the differences in the dielectric properties. The permittivity of the US gel is very different from adipose breast tissue, this causes the reference and recorded signals to be very different; therefore, we can expect the calibration procedure to lead to erroneous results in which the direct pulse and early-time response are not properly removed. In this experiment the fat-mimicking tissue has similar properties to that of the breast phantom, since the breast phantom is made to mimic purely adipose tissue. It is our expectation, and planned future work, that the calibration material should be chosen based on the breast composition; average breast permittivity can vary greatly depending on the percentage of glandular tissues. It is expected that in highly-glandular breasts the US gel would offer a better calibration medium, due to similarities in the dielectric properties. It would therefore be necessary to first obtain an estimate of the breast tissue dielectric properties. This can be calculated directly from the recorded signals; no additional measurements would be required.

A final note of interest is in regards to the use of safflower oil as a calibration material. Due to the low-loss nature of the material, it proved impossible to use in our calibration procedure. Signals travelling within the radome experienced minimal loss and proceeded to reflect off the various interfaces in the system whilst experiencing minimal attenuation. This led to data that was heavily distorted, with multiple reflections arising from the many interfaces. In fact, this result is not completely surprising - we note that in [4] a lossy saline solution was used as an immersion medium to suppress such unwanted reflections from the experimental system.

TABLE I. COMPARING TUMOUR DETECTION AND LOCALISATION FOR THE VARIOUS CALIBRATION TECHNIQUES

	SCR [dB]	Localisation Error [cm]
Differential Method	7.06	1.50
Fat-mimicking Tissue	4.59	1.49
US Gel	3.99	2.82

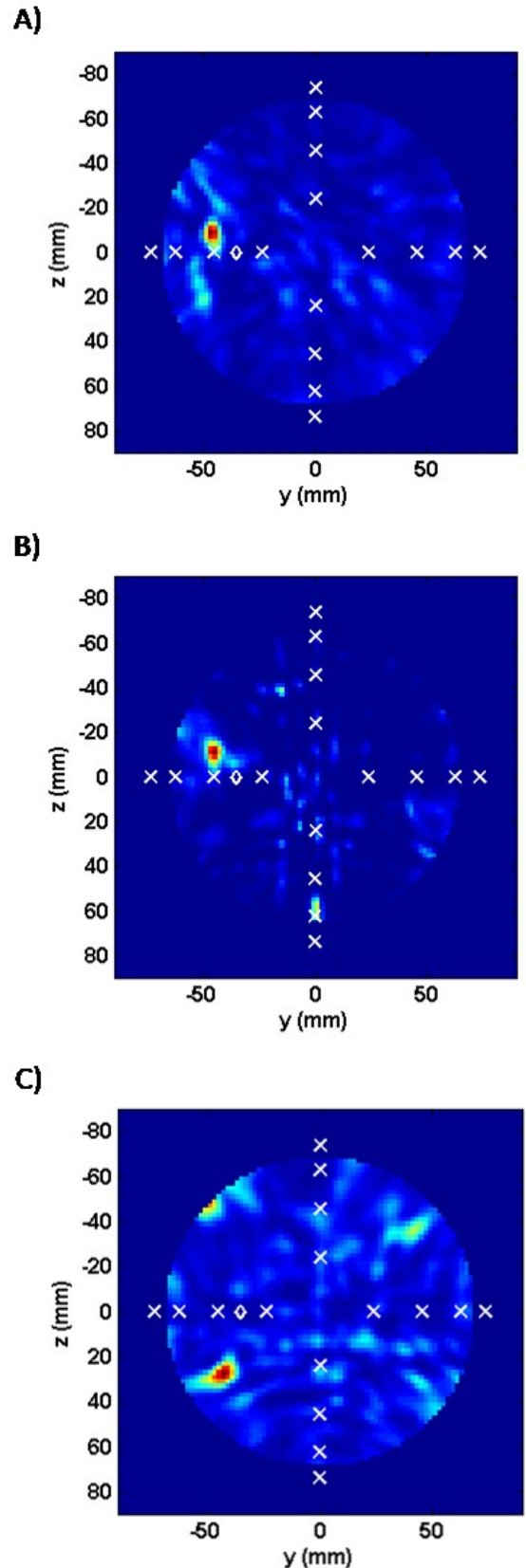


Figure 5. Comparing the reconstructed images of the breast phantoms from the various calibration methods, A) differential calibration, and the newly adopted calibration method while using B) fat-mimicking tissue, and C) US gel to obtain the reference signals.

VI. CONCLUSION

In this paper we discussed the advantages and drawbacks of a calibration technique based on recording reference signals for a time-domain microwave breast-monitoring system using various materials. We demonstrated that the main drawback of the differential calibration method, namely the need for a healthy baseline, can be avoided when using a well-chosen calibration medium. Furthermore, we have shown that the tumour detection and localisation is not negatively impacted by this new calibration technique. Future work will focus on investigating the benefits of creating a catalogue of reference signals that span a range of microwave properties such that an optimal patient-specific calibration procedure can be chosen from this signal library based on the patient's breast tissue composition.

REFERENCES

- [1] E.C. Fear, P.M. Meaney, and M.A. Stuchly, "Microwaves for breast cancer detection?," *IEEE Potentials*, pp.12-18, February/March 2003.
- [2] M. Klemm, et al., "Development and testing of a 60- element UWB conformal array for breast cancer imaging," *Antennas and Propagation (EUCAP), Proceedings of the 5th European Conference on*, pp. 3077 – 3079, Rome, Italy, Apr. 11-15, 2011.
- [3] P. M. Meaney, M. W. Fanning, D. Li, S. Poplack, and K. D. Paulsen, "A clinical prototype for active microwave imaging of the breast" *IEEE Trans Microw. Theory Techn.*, vol. 48, no. 11, Nov. 2000.
- [4] J. Bourqui, J. M. Sill, and E. C. Fear, "A prototype system for measuring microwave frequency reflections from the breast," *Int. J. Biomedical Imaging*, vol. 2012, 2012.
- [5] X. Li, E. J. Bond, B. D. V. Veen, and S. C. Hagness, "An overview of ultra-wideband microwave imaging via space-time beamforming for early-stage breast-cancer detection," *IEEE Antennas Propag. Mag.*, vol. 47, no. 1, pp. 19–34, Feb. 2005.
- [6] A. Fhager, P. Hashemzadeh, and M. Persson, "Reconstruction Quality and Spectral Content of an Electromagnetic Time-Domain Inversion Algorithm," *IEEE Trans. Biomed. Eng.*, vol.53, no.8, pp.1594-1604, Aug. 2006.
- [7] X. Zeng, A. Fhager, P. Linner, M. Persson, and H. Zirath, "Experimental investigation of the accuracy of an ultrawideband time-domain microwave-tomographic system," *IEEE Trans. Instrum. Meas.*, vol. 60, no. 12, Dec. 2011.
- [8] E. Porter, A. Santorelli, M. Coates, and M. Popović, "Time-domain microwave breast cancer detection: extensive system testing with phantoms," *Technol Cancer Res Treat.*, 2012, [Epub ahead of print].
- [9] J. C. Y. Lai, C. B. Soh, E. Gunawan, and K. S. Low, "UWB microwave imaging for breast cancer detection – experiments with heterogeneous breast phantoms," *Prog. Electromagn. Res. M*, vol. 16, pp. 19-29, 2011.
- [10] D. Byrne, M. O'Halloran, M. Glavin, and E. Jones, "Breast cancer detection based on differential ultrawideband microwave radar," *Prog. Electromagn. Res. M.*, vol. 20, pp. 231 – 242, 2011.
- [11] A. Santorelli, et al., "Experimental Demonstration of Pulse Shaping for Time-Domain Microwave Breast Imaging", *Prog. Electromagn. Res.*, vol. 133, pp. 309-329, 2013.
- [12] E. Porter, J. Fakhoury, R. Oprisor, M. Coates, and M. Popović, "Improved tissue phantoms for experimental validation of microwave breast cancer detection," in *Proc. 4th European Conference on Antennas and Propagation (EuCAP), 2010*, vol., no., pp.1-5, 12-16 April 2010.
- [13] H. Been Lim, N. Thi Tuyet Nhung, E.P. Li, and N. Duc Thang, "Confocal Microwave Imaging for Breast Cancer Detection: Delay-Multiply-and-Sum Image Reconstruction Algorithm," *IEEE Trans. Biomed. Eng.*, vol.55, no.6, pp.1697-1704, June 2008.
- [14] M. Klemm, I. J. Craddock, J. Leendertz, A. Preece, and R. Benjamin, "Radar-based breast cancer detection using a hemispherical antenna array – experimental results," *IEEE Trans. Antennas Propag.*, vol. 57, no. 6, June 2009.